International Journal of Heat and Technology
Vol. 44, No. 1, February, 2026, pp. 357-364
Journal homepage: http://iieta.org/journals/ijht

Numerical Study of DC Electric Field Effects on the Turbulent Swirl Flame in Tube Burner

Tawfeeq Kadhem Salman[1,2], Amir Musa Abazari[1], Hasanain A. Abdul Wahhab[2*]

[1] Department of Mechanical Engineering, Faculty of Engineering, Urmia University, Urmia 5756151818, Iran
[2] Training and Workshop Centre, University of Technology - Iraq, Baghdad 10066, Iraq

Corresponding Author Email: 20085@uotechnology.edu.iq

https://doi.org/10.18280/ijht.440131

Received: 20 October 2025
Revised: 18 December 2025
Accepted: 25 December 2025
Available online: 28 February 2026

Keywords:
turbulent swirl flame, DC electric field effect, ionic wind, combustion simulation, premixed combustion stability

ABSTRACT

Turbulence swirl flame structure and its stability are significant parameters for efficient combustion in industrial burners. The objective is achieved by numerical modeling and simulation using ANSYS 17.0 FLUENT Premixed Model, also called the Turbulent Flame Speed Closure (TFSC) model. The ring-plate electrode configuration was used, and the high electric potential was applied to the ring electrode as a positive electrode, while the burner edge was the negative electrode. The influence of the DC electric field on the turbulent premixed swirl flame structure and turbulent flame temperature with different values of the electric potential. The results show that the gap between the swirl flame root and burner edge decreased with increasing the applied DC electric field by 2 kV and 5 kV. Numerical results represented the increasing swirl flame temperature at 4.6% and 13.4% at the effective electric fields of 2 kV and 5 kV, respectively. The current simulation recorded good agreement with the experimental and numerical data of many studies dealing with turbulent flames.

1. INTRODUCTION

Improving the combustion process in its various forms, diffusion or premixed, within flame generators, especially in the combustion chambers of engines, aircraft turbines, and power generation plants, is a basic requirement to reduce the emission of pollutants, most notably NOx, as it includes an attempt to increase the homogeneity of the fuel-air mixture and stabilize the flame temperature. Moreover, flame instability is a problem faced by designers of modern propulsion systems [1, 2]. Pressure fluctuations and temperature instability within high ranges in closed cycles cause fluctuations in self-perpetuating reactions in the combustion chambers [3, 4]. One of the most important measures considered to develop combustion chambers and reduce emissions was controlling the combustion characteristics using a DC electric field, which may contribute to flame stability [5-7].

Numerical modeling of the interaction of a DC electric field with a flame is a very difficult topic that is rarely addressed in the literature. Research plans varied to study the effect of the electric field on the combustion field to include all the properties of laminar and turbulent flame fronts: flame structure (flame thickness, flame height, shape, changes of flame root and tip, flame stretch) [8, 9]; reduction of emissions such as CO, NOx, HC, soot [10-12]; flame stability [13, 14]; flame speed and flame temperature distribution [15, 16]; and the extent to which turbulent swirl flames are affected by ionic winds [17].

Many researchers' works have dealt with advanced numerical methods for analyzing combustion processes under the influence of an external electric field [10, 11]. Many models relied on many assumptions, for example, assuming a constant DC electric field intensity in numerical modeling [12] or relying on the transport equation for ions instead of electrons [14]. At the same time, Gan et al. [13] studied the behavior of flame front stability and focused on demonstrating the extent of the effect of the DC electric field on the emission of nitrogen oxide and trying to reduce its emission rates in combustion products. Park et al. [18] described a simplified model of flame front stability at the incinerator nozzle, where the influence of ion movement and diffusion on ion-driven winds was confirmed.

Considerable effort has gone into understanding the flame dynamics under various flow and combustor conditions, and several configurations of burner systems providing desired flame dynamics have been proposed and studied. A flame formed in the exit of tube combustors, which has a compact geometry and can be readily implemented in gas turbines and various industrial applications, is considered from the viewpoint of flame dynamics. Notably, the flame becomes stable to oscillate periodically when the supply air jet velocity exceeds a threshold value. At higher air jet velocities, however, oscillations become irregular, non-periodic, or combustion instability. A DC electric field was reported to alter flame dynamics in a tube combustor. The DC electric field can control the trajectory of charged particles, including ions, radicals, and combustion products formed near the flame, to change the geometry of the reaction zones [7]. Consequently, the flame distance from the combustor entrance and the curvature of the reaction zone are altered, which may change flame dynamics. However, how DC electric fields affect flame dynamics and combustion stability in tube combustors has not

been deeply studied.

Concepts differ in describing the effect of the electric field on the combustion region. First, the ionic wind resulting from the electric body force generates a hydrodynamic effect, the effect of which is clearly visible on the flame front [18, 19]. Secondly, the reaction enhanced by the electrons and positive ions liberated from the combustion procedure produces a chemo-kinetic effect, while the third concept includes thermal effects [20, 21]. Specifically, the relationship between the flame and the electric field depends on the concentration rate of the charged species resulting from the combustion reaction, so many factors mainly affect the concentration rates, such as the equivalence ratio of fuel-air mixtures and boundary conditions [22].

The numerical modeling and simulation of electric field interaction with the flame is a very complicated task, and few researchers have addressed it in the literature. Several research studies have dealt with the modeling of electric field interaction with the flame front. Different assumptions have been suggested in these simulations, such as depending on fixed electric field intensity in all the computational domains [23] or modeling flame under an electric field to notice flame stability [24]. Also, others focused on applying an electric field to the analysis of the nitrogen oxide emission [25, 26]. The objective of the work is to study the ability of electric fields to affect flame stability and also to give a descriptive approach to the effect of the electric charge on the flame, which is then presented and validated. The swirl flames of LPG/air are used to analyze the dynamics of stabilization of the flame extremity in the presence of an applied electric field.

2. NUMERICAL ANALYSIS

2.1 Physical description

The chemical basis describes the extent to which the electric field affects the behavior of fire within the combustion process due to the presence of ionic species. Much literature has dealt with the effect of the electric field on the flame in order to improve the flame properties, starting with flame speed and stability, flame front brightness, flame composition, and pollutant emissions. Moreover, it verified the possibility of electric fields being considered one of the flame control triggers. As a result of the electron transfer or ionization accompanying the collision process or chemical ionization, ions are formed in the flame. Schmidt [27] reported that the reaction in hydrocarbon's combustion process was a reason for the production of H_3O^+ ion. While the reaction produces CHO^+ ion [27]:

$$CH + O \rightarrow CHO^+ + e^- \quad (1)$$

$$CHO^+ + H_2O \rightarrow CO + H_3O^+ \quad (2)$$

While H_3O^+ is involved in another reaction [27];

$$H_3O^+ + e^- \rightarrow H_2O + H \quad (3)$$

Figure 1 demonstrates the effect of the electric field applied to the flame; firstly, the Coulomb force generated by an electric field is the force affecting electric charges placed within the range of this field. As shown in the figure, the electric field affected by the combustion region moves electrons from the reaction region to the positive electrode. In contrast, the positive ions move in the opposite direction. When positive ions collide with the natural species, part of the ions' momentum is transferred to the natural species, thereby generating a hydrodynamic pressure on the flame front. It is called the ionic wind.

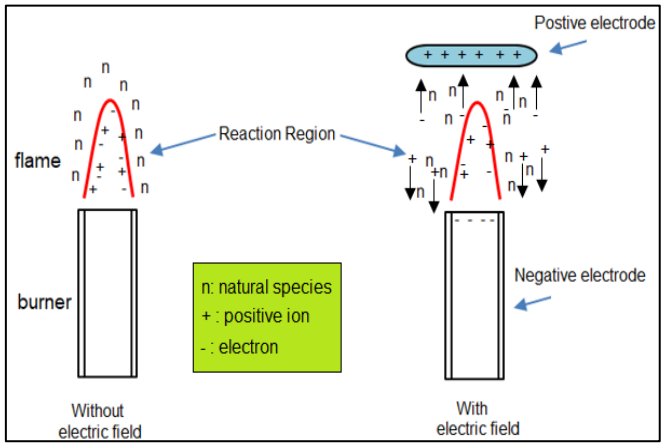

Figure 1. The schematic of the ionic wind generated in the flame front

2.2 Computational methodology

A model of Turbulent Flame Speed Closure (TFSC) was adopted to simulate the swirl combustion for turbulent flame in a vertical burner under the effect of a DC electric field. Modeling was also completed within an environment of the commercial Computational Fluid Dynamics (CFD) software ANSYS 17.0 FLUENT, for premixed combustion. The combustion of swirl turbulent flame under the effect of an electric field, including the low swirl formation premixed in the lean side, was simulated by Fluent. The electric field equation was applied in Fluent by User Defined Function (UDF) and contacted with the simulation by UDFs, which were prepared in C++. Several steps were used for performing the simulations, as shown in Figure 2. This simulation investigates the influence of DC electric fields on the low swirl flame through an edge burner.

The 3D model of a vertical burner was prepared in SolidWorks 10.0 software and adapted to analyze the swirl flame structure and stability for a premixed turbulent swirl flame under a range of DC electric fields at LPG/air flame. The turbulent swirl flame model comprises two zones. The dimensions of the first zone, the vertical burner, were received from the experimental setup for Abdul Wahhab [4]. A vertical burner includes a pipe of 42 mm in inner diameter and 500 mm in length, 30 mm from the external edge of the burner. As shown in Table 1, four strips were fixed inside the burner. These strips were welded in a helical path to generate a swirl flow pattern for the premixed gases while identifying the angle between the plate's axes at 90°, as shown in Figure 3. The second zone includes a reaction region, or swirl flame zone, meaning that the flame speed possesses a tangential and axial component. The tangential component of velocity is generated by inter-burner strips (having an outlet angle of 90°) to the axial direction. The second zone includes the electrode ring with a diameter of 90 mm located at 110 mm above the burner edge, and a high electric potential was applied to the ring electrode as the positive electrode, while the burner edge represents the negative electrode.

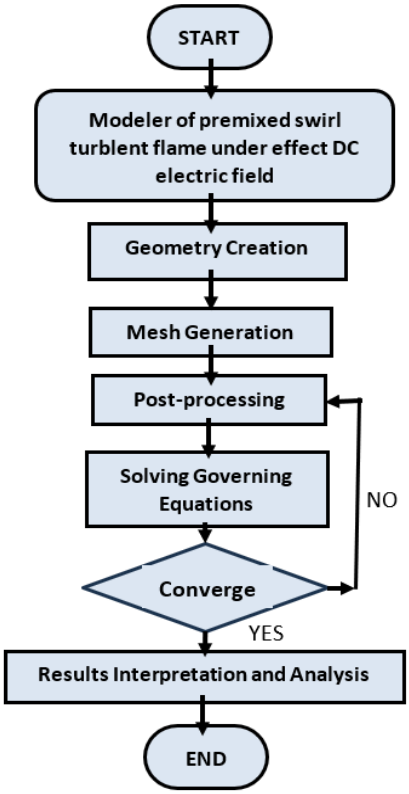

Figure 2. Flow chart of simulation steps

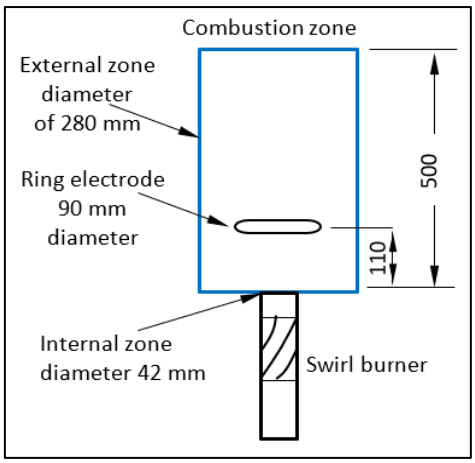

Figure 3. Sketch of swirl burner domain geometry

Table 1. Swirl burner geometric dimensions

Parameter	Value
Internal zone diameter (d)	42 mm
External zone diameter	280 mm
External zone height	500 mm
Ring electrode diameter	90 mm
Ring electrode height from burner edge [*l*]	110 mm

The computational grid is a critical component of the simulation process. It's a discretization of the geometric domain of the problem into smaller, manageable elements or cells. This grid forms the basis on which numerical methods solve the combustion equations. Meshing is a crucial step for defining the computational domain and ensuring accurate and efficient simulation results. Types of meshing can be broadly categorized based on element shape, structure, and method. In this research, air-fuel mixture flow and combustion domain are meshed with adopting tetrahedral, structure-based, and path-conforming meshing because they generally provide higher accuracy and efficiency for certain simulations, have a regular grid structure with well-defined layers, are suitable for complex geometries with multiple faces and regions, and maintain the integrity of the original geometry. Computational processes have been carried out for four selected grid sizes: 145620, 280630, 415630, 623451, and 788467. A summary of the grid-independent test results is shown in Table 2. Observed that the 623451 and 788467 nodes produced almost identical results. Hence, a domain with 788467 nodes was chosen to increase computational accuracy and reduce the time of computation. Figure 4 shows the variation of average time with the total element number. Results for the selected grid sizes show very good agreement with each other.

Table 2. Grid independence test result

No.	Number of Nodes	Number of Elements	Temperature (K)
1	145620	95788	1498
2	280630	115678	1415
3	415630	278944	1378
4	623451	467782	1245
5	788467	697833	1239

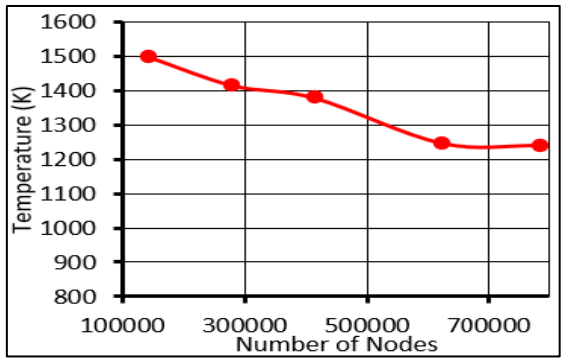

Figure 4. Variation of average time with total element number

Table 3. Important parameters of the computational model

Parameter	Value
Applied Electric Potential (V)	0, 2, and 5 kV
Premixed LPG/air flame	
n-Butane	12.5% w/w
Isobutane	17.5% w/w
Propane	70% w/w
Equivalent ratio (ϕ)	0.7
Inlet boundary conditions	
LPG (axial velocity)	0.85 m/s
Air (axial velocity)	10.4 m/s
Density	
LPG	0.884 kg/m^3
Air	1.184 kg/m^3
Turbulent kinetic energy (m^2/s^2)	1.64

The mesh of the geometry appears in Figure 5. The number of nodes and elements is 788467 and 697833, respectively. The ANSYS Design Modeler was used to make the geometry model, while the fine meshing tool was used to prepare the mesh body. A grid independent test was performed to ensure that the mesh sizes are considered to produce identical results. The mesh size is refined at the fuel-air mixture inlet to get the

most accurate numerical results. The important parameters of simulations are demonstrated in Table 3.

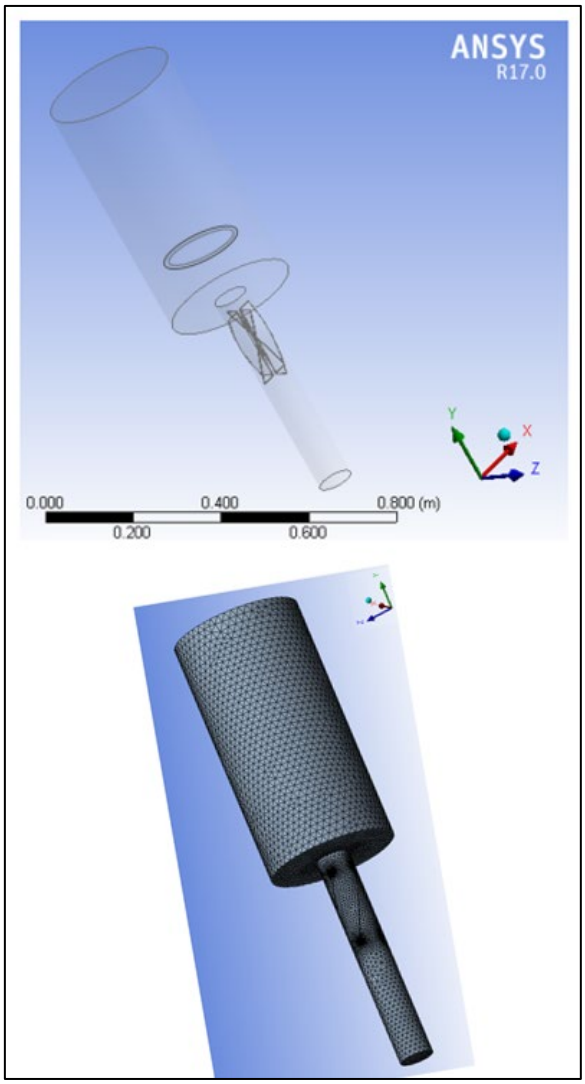

Figure 5. Computational domain and geometrical mesh model of a vertical tube burner

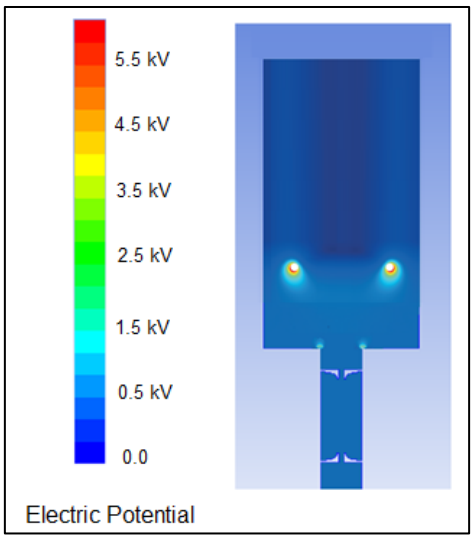

Figure 6. Distribution of electric field intensity without flame

The electric potential is generated between the burner outlet and the ring electrode. To get a clear idea of the electric field effects, the simulation without combustion was done first to verify the effect of electric field dissuasion in the reaction region by ANSYS 17.0, as shown in Figure 6. The electric field gradient points are generated from the ring electrode to the burner edge.

2.3 Governing equations

The CFD model was controlled by a number of assumptions.

- Unsteady, two dimensions, premixed swirl flame in the external region.
- Low swirl rate of mixed gases in the internal region, also the homogeneously assumed that LPG/air together, that the LPG to air ratio is of the order of limitation, and evaporation, initial reaction phenomena can be neglected.
- Assume a steady DC electric field. An important process that happens in addition to ionization is the recombination process.
- Assume no reactions between LPG gas and air in the internal burner region. Furthermore, assuming that gases (LPG and air) are adopted as two reactants and their properties remain constant.

The dynamic fluid equations for fuel mixtures, multi-vector, compressible fluid, and dynamic flows with the influence of electric forces control the subject. Where ρ is a mixture of density v_i is the mixture of velocity components, and F_i is the external electric force, the mass continuity and momentum equations read [5]:

$$\frac{\partial \rho}{\partial t} + \frac{\partial \rho v_i}{\partial x_i} = 0 \tag{4}$$

$$\frac{\partial \rho v_i}{\partial t} + \frac{\partial \rho v_i v_j}{\partial x_i} = -\frac{\partial p}{\partial x_i} + \frac{\partial \tau_{ij}}{\partial x_i} + F_i \tag{5}$$

where, t is time, and x_i is the typical coordinates. p is total pressure, and τ_{ij} is the viscous tensor [5]:

$$\tau_{ij} = -\frac{2}{3}\mu \frac{\partial \rho v_k}{\partial x_k}\delta_{ij} + \mu\left(\frac{\partial v_i}{\partial x_j} + \frac{\partial v_j}{\partial x_i}\right) \tag{6}$$

where, μ is the dynamic viscosity and $\delta_{i,j}$ *is* the Kronecker factor.

The vectors of the electric force F_i that is generated from charge boosters when a DC electric field is affected by applied electric field intensity E_i and charge boosters' types n^+, n^- [5]:

$$F_i = eE_i(n^+ - n^-) \tag{7}$$

where, the n^- and n^+ are negative and positive charge boosters, also, e represents the transported electron. At the same time, the intensity of the electric field is calculated from the electric potential V by the simple equation [5].

$$E_i = -\frac{\partial V}{\partial x_i} \tag{8}$$

The electric potential is divided as described by the Poisson equation, which changes in time with active species concentrations, and ε_o represents the permittivity of the free region.

$$\nabla^2 V = -e\frac{(n^+ - n^-)}{\varepsilon_o} \tag{9}$$

Chemical species equations (neutral or charged) could be presented by Eq. (10) [5]:

$$\frac{\partial \rho Y^k}{\partial t} + \frac{\partial \rho v_j Y^k}{\partial x_i} = -\frac{\partial \rho Y^k V_j^k}{\partial x_i} + \dot{\omega}^k \quad (10)$$

The energy equation can present:

$$\frac{\partial \rho E}{\partial t} + \frac{\partial \rho v_i E}{\partial x_i} = -\frac{\partial q_i}{\partial x_i} + \frac{\partial (\tau_{ij} - p\delta_{ij})}{\partial x_i} + \dot{Q} + f \quad (11)$$

where, f, the energy transport equation by contribution to the electric force, is known as:

$$f = \sum_{k=1}^{Nc} en^k S^k E_j \left(v_j + V_j^k\right) \quad (12)$$

3. RESULTS AND DISCUSSION

The influence of the DC electric field on a stabilized turbulent swirl flame was analyzed. In the first case, the LPG and air flow rates were applied to get on lean side mixing at an equivalent ratio of 0.7, without DC electric field to record swirl flame behavior at these conditions to determine the characteristics of the flame vortex: its height, increasing in the vortex's diameters, and the amount of gap separating it from the edge of the burner. In the subsequent cases, electric fields were applied at 2 kV and 5 kV, respectively, at the same mixing conditions for the flame vortex. Figure 7 demonstrates the mass fraction contours of burning gases for the flame vortex at different DC electric fields applied. As shown in the figure, the electric field strongly affects the vortex flame behavior. This is evident by reducing the separation limit between the root of the flame vortex and the edge of the burner when an electric field of 5 kV is applied, while a clear decrease in the diameter of the flame vortex can be observed at the upper end of the flame when an electric voltage is applied. I.e., the turbulent swirl flame translated toward the edge burner, the ionic winds generated are responsible for this behavior. These results are consistent with many experimental studies that confirmed the increased stability of turbulent flames under the influence of an electric field [1, 7].

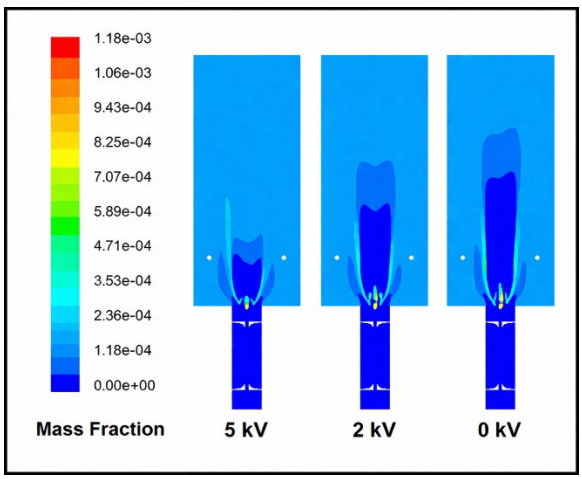

Figure 7. Mass fraction contours of burning gases for vortex flame at different DC electric fields applied: 0, 2, and 5 kV

In order to study the effect of the DC electric field on the vortex flame temperature, a turbulent swirl flame under an equivalence ratio of 0.7 was selected to be analyzed. Figure 8 shows the contours of vortex flame temperatures above the burner edge under the effect of different electric fields. Generally, the temperature of a turbulent swirl flame changes depending on three regions in the vortex flame: the preheating region, the first reaction region, and the second reaction region. The higher values of temperature in the turbulent swirl flame appear in the first reaction region. In contrast, the flame temperature increased with the increasing electric potential. The movements of ions in a swirl flame enhanced the combustion process, resulting in higher flame temperatures under the effect of a DC electric field. These results are in agreement with the experimental results of Li et al. [1].

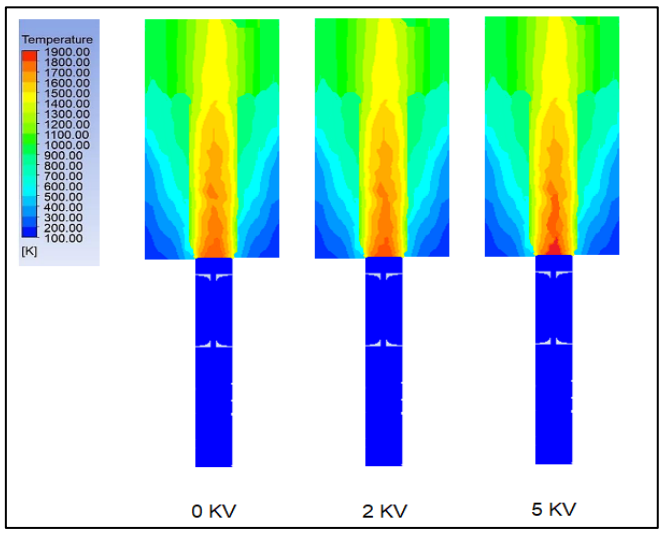

Figure 8. Flame temperature contours on the swirl burner under different electric fields

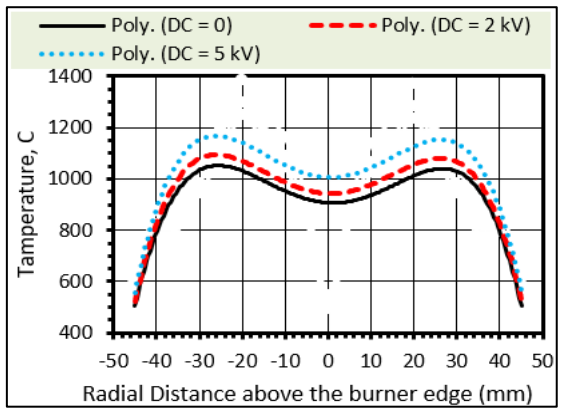

Figure 9. Flame temperature distribution at an equivalent ratio of 0.7 under different electric fields

Figure 9 shows the distribution of vortex flame temperatures with radial distance above the burner edge under the effect of different electric fields. The figure shows swirl flame temperature distribution for equivalence ratios 0.7, demonstrating the various reactions to changes in different electric fields, 2 and 5 kV of the swirl flow planar flame along 100 mm axial distance in mid-distance above the burner edge. Here, 4.6% is indicated as the increased percentage with the effect of a 2 KV electric field, while 13.4% is represented as a higher percentage because of an increased electric field to 5 KV. The temperature distribution is approximately cylindrically symmetric with hotter borders. With a positive

DC field, the center spot temperature is lower, and the profile is higher, while the increased field case has a higher temperature and narrower profile. The small aberrations on the sides of the peak in the profiles occur because of the weak ionic wind effect in these regions and give variations of local emissivity. This data suggests that the heat transfer rate above the flame front can be changed or modified by the DC electric field, and, more so, controlled combustion under the influence of electric fields may increase heat transfer through the working environment.

The numerical results showed the direct effect of the DC electric field on the emission of soot particles. Figure 10 shows that increasing the distance between the two electrodes in the DC electric field has a significant effect on the production of soot particles. It turns out that as the distance between the electrodes increases relatively, the scaling of the DC electric field on the soot particles is greater, and this behavior is consistent with the research results of many researchers [24, 26-28] who described the physical explanation. Experimental emission samples of the soot particles under a variable intensity electric field were studied. This is done by inducing ionic winds to carry charges under an electric field, which certainly affects the path of the soot particles and the movement of the interacting liquid medium. In general, ionic winds are considered the main cause of the geometric change of the flame front due to the acceleration of the charged species and the increase in the burning rate. The effect of the electric field on the combustion growth mechanism is the main source of the variation in soot formation in the flame.

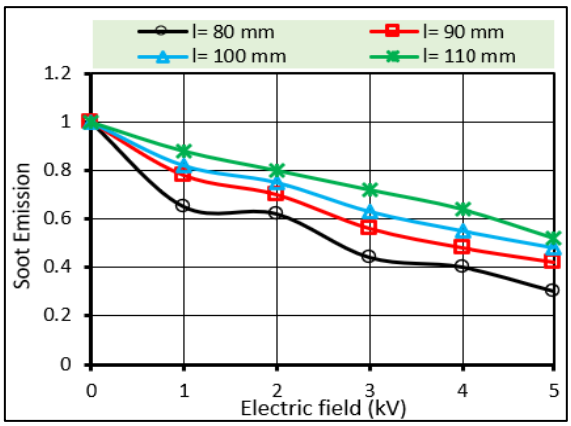

Figure 10. Changes in the mass concentration of soot particles in a DC electric field

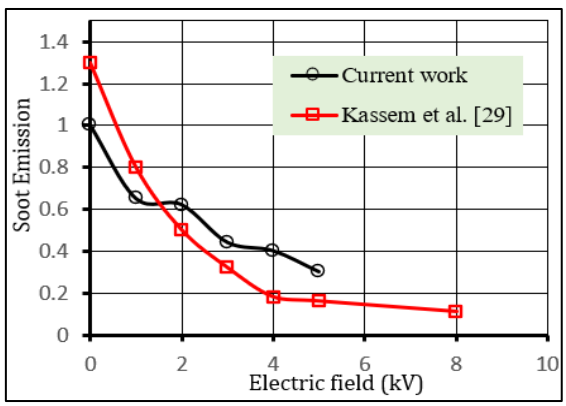

Figure 11. Comparison of numerical results with experimental results [29]

The modification of the flame geometrical due to the ionic winds increased the acceleration of charged species and the burning rate. Generally, simulated results compared with experimental results for Kassem et al. [29], when a DC electric field of 1 to 8 kV was applied, the flame appeared to be shorter and larger, as shown in Figure 7. Also, soot emission decreased due to the particles' volume increasing under the effect of the electric field. The results appear in Figure 11.

4. CONCLUSIONS

The turbulent swirl flame from a tube burner using LPG as fuel with air at an equivalent ratio of 0.7 (lean fuel side) under a DC electric field was studied numerically. The effects of a DC electric field on swirl flame stability and flame temperature were investigated. The main conclusions are summarized as follows: The distance between the swirl flame root and burner edge decreased with increasing applied DC electric field due to the ionic wind effect, which in turn increases the flame temperature and the diffusivity. Numerical results were represented by the increasing swirl flame temperature at 4.6% and 13.4% at the effect of electric fields 2KV and 5 kV, respectively. The application of DC electric fields can reduce the emission of soot particles, and the effect of the small distance between DC electrodes is better. Particle diagnosis technology needs to be further developed to obtain more accurate values and observe more subtle changes. Future works by the researchers must include studying a wide range of electric potential with flame properties and more stable combustion rates. A numerical study on the influence of DC electric field on the flame front in swirl flame should be performed to describe the combustion mechanism quantitatively.

ACKNOWLEDGMENT

The authors acknowledge the University of Technology-Iraq for its support in conducting the research and producing this paper.

REFERENCES

[1] Li, Y., Wang, J., Xia, H., Ju, R., Yu, J., Mu, H., Huang, Z. (2023). Effect of DC electric field on turbulent flame structure and turbulent burning velocity. Combustion Science and Technology, 195(2): 692-712. https://doi.org/10.1080/00102202.2021.1969376

[2] Mola, A.H., Abdul Wahhab, H.A., Naji, Z.H. (2023). Effects of nozzle diameter and number of carbon atoms in fuel on flame quenching in counter burner. In Lecture Notes in Mechanical Engineering. https://doi.org/10.1007/978-981-19-1939-8_11

[3] Abdul Wahhab, H.A. (2021). Investigation of stability limits of a premixed counter flame. International Journal of Automotive and Mechanical Engineering, 18(1): 8540-8549. https://doi.org/10.15282/ijame.18.1.2021.13.0648

[4] Abdul Wahhab, H.A. (2023). Influence of swirl flow pattern in single tube burner on turbulent flame blow-off limit. In Lecture Notes in Mechanical Engineering. https://doi.org/10.1007/978-981-19-1939-8_2

[5] Guo, L., Zhai, M., Shen, Q., Guo, H., Dong, P. (2021). Effect of hydrogen addition on the ionization of partially premixed methane flame. Fuel, 285(1): 119141. https://doi.org/10.1016/j.fuel.2020.119141
[6] Khlaf, A.M., Ehyaei, M.A., Abdul Wahhab, H.A. (2023). CFD simulation of premixed flame in counter burner under the influence of a magnetic field. International Journal of Computational Methods and Experimental Measurements, 11(4): 233-238. https://doi.org/10.18280/ijcmem.110404
[7] Khlaf, A.M., Abdul Wahhab, H.A., Ehyaei, M.A. (2023). Impact of magnetic field on the stability of laminar flame in a counter burner. International Journal of Energy Production and Management, 8(4): 229-234. https://doi.org/10.18280/ijepm.080404
[8] Wang, J., Yu, Q., Zhang, W.M., Huang, Z. (2019). Development of a turbulence scale controllable burner and turbulent flame structure analysis. Experimental Thermal and Fluid Science, 109: 109898. https://doi.org/10.1016/j.expthermflusci.2019.109898
[9] Duan, H., Li, Z., Wang, B., Mehra, R.K., Luo, S., Xu, C., Sun, B., Wang, X., Ma, F. (2019). Experimental study of premixed hydrogen enriched natural gas under an alternating-current (AC) electric field and application of support vector machine (SVM) on electric field assisted combustion. Fuel, 258(15): 115934. https://doi.org/10.1016/j.fuel.2019.115934
[10] Guo, L., Zhai, M., Shen, Q., Guo, H., Dong, P. (2021). Effect of hydrogen addition on the ionization of partially premixed methane flame. Fuel, 285: 119141. https://doi.org/10.1016/j.fuel.2020.119141
[11] Zhang, Y., Wu, Y., Yang, H., Zhan, H., Zhu, M. (2013). Effect of high-frequency alternating electric fields on the behavior and nitric oxide emission of laminar non-premixed flames. Fuel, 109: 350-355. https://doi.org/10.1016/j.fuel.2012.12.083
[12] Park, D.G., Choi, B.C., Cha, M.S., Chung, S.H. (2014). Soot reduction under DC electric fields in counterflow non-premixed laminar ethylene flames. Combustion Science and Technology, 186(4-5): 644-656. https://doi.org/10.1080/00102202.2014.883794
[13] Gan, Y.H., Luo, Y.L., Wang, M., Shi, Y.L., Yan, Y.Y. (2015). Effect of alternating electric fields on the behaviour of small-scale laminar diffusion flames. Applied Thermal Engineering, 89: 306-315. https://doi.org/10.1016/j.applthermaleng.2015.06.041
[14] Gillon, P., Gilard, V., Idir, M., Sarh, B. (2019). Electric field influence on the stability and the soot particles emission, of a laminar diffusion flame. Combustion Science and Technology, 191: 325-38. https://10.1080/00102202.2018.1467404
[15] Zhen, H., Wang, Z., Liu, X., Wei, Z. Huang, Z., Leung, C. (2020). An experimental study on the effect of DC electric field on impinging flame. Fuel, 274: 117846. https://doi.org/10.1016/j.fuel.2020.117846
[16] Duan, H., Wu, X., Sun, T., Liu, B., Fang, J., Li, C., Gao, Z. (2015). Effects of electric field intensity and distribution on flame propagation speed of $CH_4/O_2/N_2$ flames. Fuel, 158: 807-815. https://doi.org/10.1016/j.fuel.2015.05.065
[17] Li, Y., Wang, J., Xia, H., Li, C., Zhang, M., Wu, X., Huang, Z., Mu, H. (2018). Effect of DC electric field on laminar premixed spherical propagation flame at elevated pressures up to 0.5 MPa. Combustion Science and Technology, 190(11): 1900-1922. https://doi.org/10.1080/00102202.2018.1467407
[18] Park, D.G., Chung, S.H., Cha, M.S. (2017). Visualization of ionic wind in laminar jet flames. Combustion and Flame, 184: 246-248. https://doi.org/10.1016/j.combustflame.2017.06.011
[19] Kuhl, J., Seeger, T., Zigan, L., Will, S., Leipertz, A. (2017). On the effect of ionic wind on structure and temperature of laminar premixed flames influenced by electric fields. Combustion and Flame, 176: 391-399. https://doi.org/10.1016/j.combustflame.2016.10.026
[20] Kuhl, J., Jovicic, G., Zigan, L., Will, S., Leipertz, A. (2015). Influence of electric fields on premixed laminar flames: Visualization of perturbations and potential for suppression of thermoacoustic oscillations. Proceedings of the Combustion Institute, 35(3): 3521-3528. https://doi.org/10.1016/j.proci.2014.08.026
[21] Luo, Y., Gan, Y., Jiang, X. (2017). Investigation of the effect of DC electric field on a small ethanol diffusion flame. Fuel, 188: 621-627. https://doi.org/10.1016/j.fuel.2016.10.073
[22] Zhang, M., Wang, J., Xie, Y., Wei, Z., Jin, W., Huang, Z., Kobayashi, H. (2014). Measurement on instantaneous flame front structure of turbulent premixed CH_4/H_2/air flames. Experimental Thermal and Fluid Science, 52: 288-296. https://doi.org/10.1016/j.expthermflusci.2013.10.002
[23] Luo, Y., Gan, Y., Jiang, Z. (2018). An improved reaction mechanism for predicting the charged species in ethanol-air flame. Fuel, 228: 74-80. https://doi.org/10.1016/j.fuel.2018.04.157
[24] Obaid, L.T., Abdul Wahhab, H.A., Chaichan, M.T., Fayad, M.A., Al-Sumaily, G.F. (2023). Influence of burner diameter on premixed flame shape and quenching. International Journal of Computational Methods and Experimental Measurements, 11(4): 245-250. https://doi.org/10.18280/ijcmem.110406
[25] Wang, Y., Sharma, G., Koh, C., Kumar, V., Chakraharly, R., Biswas, P. (2017). Influence of flame-generated ions on the simultaneous charging and coagulation of nanoparticles during combustion. Aerosol Science and Technology, 51(7): 833-844. https://doi.org/10.1080/02786826.2017.1304635
[26] Sakhrieh, A., Lins, G., Dinkelacker, F., Hammer, T., Leipertz, A., Branston, D.W. (2005). The influence of pressure on the control of premixed turbulent flames using an electric field. Combustion and Flame, 143(3): 313-322. https://doi.org/10.1016/j.combustflame.2005.06.009
[27] Schmidt, J., Ganguly, B. (2013). Effect of pulsed, sub-breakdown applied electric field on propane/ air flame through simultaneous OH/acetone PLIF. Combustion and Flame, 160(12): 2820-2826. https://doi.org/10.1016/j.combustflame.2013.06.031
[28] Al Asfar, J., Alkhalil, S., Sakhrieh, A., Al-Domeri, H. (2018). 2-D numerical modeling of flame behavior under electric field effect. International Journal of Heat and Technology, 36(3): 1101-1016. https://doi.org/10.18280/ijht.360342
[29] Kassem, A.S., Gillon, P., Idir, M., Gilard, V. (2019). On the effect of a DC electric field on soot particles' emission of a laminar diffusion flame. Combustion Science and Technology, 194(1): 213-224. https://doi.org/10.1080/00102202.2019.1678901

NOMENCLATURE

CFD	Computational Fluid Dynamics
CD	electric fields
LPG	liquid petroleum gas
Fi	the electric body force, N
Ei	the electric field intensity, N/C
t	time, sec
v	flow velocity component, m/sec
V	electric potential, kV
$n+, n-$	charged species concentrations, mol/L
f	the electric force contribution
P	static pressure, Pa
e	the electron charge, coulomb
d	internal zone diameter, mm
T	temperature, ℃
t	time, s
Q	turbulent kinetic energy, m^2/s^2
x	cartesian coordinates, m
l	ring electrode height from burner edge, mm

Greek symbols

α	thermal diffusivity, $m^2 \cdot s^{-1}$
β	thermal expansion coefficient, K^{-1}
ε	worn stainless steel's emissivity
ρ	density, kg/m^3
μ	dynamic viscosity, kg. $m^{-1} \cdot s^{-1}$
ρ	density, kg/m^3
εo	the permittivity of free space
ϕ	equivalent ratio
ν	kinematic viscosity, m^2/s
μ	dynamic viscosity, Pa·s
δ	the kronecker symbol